Automation in Construction 89 (2018) 49–57

Contents lists available at ScienceDirect

Automation in Construction

journal homepage: www.elsevier.com/locate/autcon

Assessment of the feasibility of detecting concrete cracks in images acquired by unmanned aerial vehicles

Xingu Zhong*, Xiong Peng, Shengkun Yan, Mingyan Shen, Yinyin Zhai

Hunan University of Science and Technology, Xiangtan 411100, Hunan, China

ARTICLE INFO

Keywords:
Unmanned aerial vehicle
Image recognition
Crack width

ABSTRACT

An 8-rotor unmanned aerial vehicle is used as a working platform. Its motion characteristics in a hovering state are obtained using a non-contact measurement instrument, which, along with the modulation transfer function of its airborne images, indicates the reliability of the airborne images of unmanned aerial vehicles in a hovering state. By installing a laser range finder on the cradle synchronized with the camera shutter to measure the object distance, the pixel resolution of the object distance is obtained. The airborne images are then processed using the MATLAB image processing toolbox, from which the pixels of concrete cracks are extracted. Compared to a static image and direct manual measurements, the airborne image of the unmanned aerial vehicle has higher precision, indicating its wide potential applications as an alternative of the conventional inspection methods of bridge-inspection vehicle and working platforms.

1. Introduction

The crack width of concrete structures is one of the most crucial parameters in evaluating a structure's performance and conditions. Recent years have observed the rapid development of image-based crack identification research on fixed or handheld image devices [1]. XIAO Chunxia et al. [2] used the Gaussian mixture model to evaluate the image level set function, implementing crack image auto-segmentation. FANG Zhi et al. [3] proposed the attachment of solid color calibration modules on concrete surfaces to calibrate and correct the raw image of test surfaces that are not perpendicular to the camera's optical axis. The results indicated that the precision of crack width identification by orthogonal and angled images was 93.4% and 90.9%. Bang Yeon Lee et al. [4] pre-processed and ran crack identification on an uneven illuminated image based on the morphology, introducing calculation methods of crack width, length and direction, and identified crack modes in an artificial neural network. Hoang-Nam Nguyen et al. [5] used isotropic undecimated wavelet transform (IUWT) and morphological image processing for crack identification. Reference [6] used Otsu's method and multiple filtering techniques in image processing to change the image grayscale, and used image filtering and edge detection of the Sobel operator to obtain the crack width. Jieh-haur chen [7] used the image processing technique of self-organizing mapping (SOMO) to detect the Hsichou Bridge, which verified the feasibility of the Bridge detection based on image processing technology. In tunnel detection, the techniques of crack recognition on the use of image are also studied [8–9]. With the support of the Robo-spect project, Loupos [10–11] developed the autonomous robot platform and used the machine vision to detect the tunnel and complete the experiment test in the Egnatia motorway tunnel. Protopapadakis et al. used the convolution neural network (CNN) technology to perform visual inspection, evaluation and maintenance of the tunnel. Based on image processing and deep learning model, tunnel defect feature is obtained to realize automatic tunnel detection [12–19].Although there have been certain achievements in image-based crack identification research, few practical applications are present. The main reason is that fixed or handheld image devices and crack width measurement instruments require the building of support platforms for direct measurement of crack width. For the inspection of a bridge's structure, it requires a special bridge inspection car platform, which takes up nearly two lanes and greatly affects traffic. Compared to the above image based crack identification methods using fixed or handheld image devices, the manual measurement of crack widths is faster and more straightforward under the same conditions.

Recent years have also seen extensive national and international civil applications of unmanned aerial vehicles in aerial photography, geological surveys, high voltage line inspection, oilfield pipeline inspection, highway administration, forest fire patrol, toxic gas inspection, drug detection, emergency rescue, ambulance, agriculture and so on [20–28]. Unmanned aerial vehicles have also been applied in the physical inspection of civil engineering. The Aerobi EU project has been established in Europe aims at the development and validation of the

* Corresponding author.
E-mail address: 1020086@hnust.edu.cn (X. Zhong).

https://doi.org/10.1016/j.autcon.2018.01.005
Received 23 September 2016; Received in revised form 19 December 2017; Accepted 10 January 2018

prototype of an innovative, intelligent, aerial robotic system. Sanchez-Cuevas and Moliard et al. designed the unmanned aerial vehicle's systems of the Bridges detection [29–30]. Fabio Celestino, S. Sankarasrinivasana and E. Hallermann et al. [31–33] conducted a structure appearance inspection through remote control of an unmanned aerial vehicle equipped with a high-resolution video camera, obtaining appearance images of a water tower and castle but without crack width identification. Long Wang [34] used the unmanned aerial vehicle to detect the blades of the wind turbine, used the Haar transform and SVM (Support Vector Machine) to identify the blade crack, count the number of cracks and determine their position in the original image. Ellenberg [35] built the interior model beam to simulate the actual bridge disease situation. He tested the model beam with a small UAV and obtained the appearance image of simulated disease. Unmanned aerial vehicles, as an alternative of scaffolding and bridge inspection car platforms, can conduct inspections of concrete surface defects, crack shapes, width and so on through airborne devices and remote controls, solving existing problems associated with conventional work platforms. This paper obtains the image quality evaluation criteria of an airborne image by testing the motion characteristics of an unmanned aerial vehicle in a hover state, and conducts crack width identification with an airborne static image. The results are compared with the direct measurement of crack width, which indicates the reliability, practicality and potential application of crack width identification using an airborne image from an unmanned aerial vehicle.

2. Image processing and concrete crack width identification

Fig. 1 shows the workflow of concrete crack width identification based on the real-time measurement of the object distance and the functions of the MATLAB image processing toolbox.

2.1. Pixel resolution

A three-point laser range finder is installed on the cradle of the unmanned aerial vehicle and synchronized with the camera shutter to measure the object distance at the same time. According to the principle of lens imaging,

$$\frac{1}{L'} + \frac{1}{L} = \frac{1}{f} \Rightarrow L' = \frac{Lf}{L-f} \tag{1}$$

In Eq. (1), L' is the image distance; L is the object distance, namely the distance between the range finder and the target; and f is the lens focus. We assume A is the actual size of target, namely the crack's actual physical width and A' is the image size:

$$\frac{A'}{A} = \frac{L'}{L} \Rightarrow A = \frac{L}{L'}A'. \tag{2}$$

We combine Eq. (1) and Eq. (2) and obtain the following:

$$A = \frac{L-f}{f}A'. \tag{3}$$

The image size A' can be expressed as follows:

$$A' = \frac{d}{D} \times A''. \tag{4}$$

In Eq. (4), A'' is the number of pixels in the image, d is the physical size of the long side of the image sensor, and D is the number of pixels in the long side of the image sensor. The relation between the actual size$A$and image pixelsA'' can be expressed as follows:

$$A = J \cdot A''. \tag{5}$$

In Eq. (5), $J = \frac{(L-f)\cdot d}{f \cdot D}$. It is the pixel resolution, which indicates the actual physical size represented by a unit pixel and serves as the conversion coefficient between the actual physical size and number of pixels. We conduct a series of processing of the digital image, and obtain the pixels of the target in the overall image. We then calculate the actual physical size of the target (cracks) according to Eq. (5).

2.2. Image processing

Images of a concrete surface crack on the fence wall of the stadium from the author's institute are captured by a static camera, as shown in Fig. 2. According to the workflow in Fig. 1, based on MATLAB image processing tools, the enlarged areas of the colored image in Fig. 2 are normalized in post-processing, resulting in grayscale images shown in Fig. 3. The pixel grayscale histogram modification method is adopted in Fig. 3 for image enhancement, which best separates the crack from background, and turned into Fig. 4. Because of the fact that the concrete crack edges are very complicated curves and that there could be holes or material deficiencies along the cracks, the signal-to-noise ratio (SNR) of the image is increased after image enhancement, requiring median filtering of Fig. 4 to obtain Fig. 5. Through image enhancement and filtering in the spatial domain, the contrast between the crack and concrete surfaces becomes more evident. The gray level of the crack area in the crack images in Fig. 5 is small, but the gray level of the concrete background area is large. The threshold segmentation then separates the crack area from the background of concrete. This causes the result that the crack area becomes black and background of concrete becomes white, as shown in Fig. 6. If there are watermarks and other defects that are close to the background gray of concrete, they can also be separated from the cracks in the threshold segmentation. The crack area becomes black, while the concrete background and watermarks et al., which are close to the concrete background become white. After threshold segmentation, the concrete surface defects, such as porosity, holes or honeycombs and mark lines of marker, become black as cracks. All black targets in the image are marked after threshold segmentation. The number of pixels and coordinates of each marked area are counted, and the maximum coordinate difference as well as the maximum coordinate value and the area are calculated. After threshold segmentation, the concrete surface defects, such as porosity, holes or honeycombs and mark lines of marker, become black like cracks, which is shown in Fig. 6. Taking the number of pixels in marked areas as the threshold, the noises of “isolated points” or “isolated blocks can be eliminated through a morphological operation of the binary image, as shown in Fig. 7.Based on Fig. 7, the number of pixels in the cracks can be obtained. Based on the pixel resolution, the actual physical crack width can be calculated.

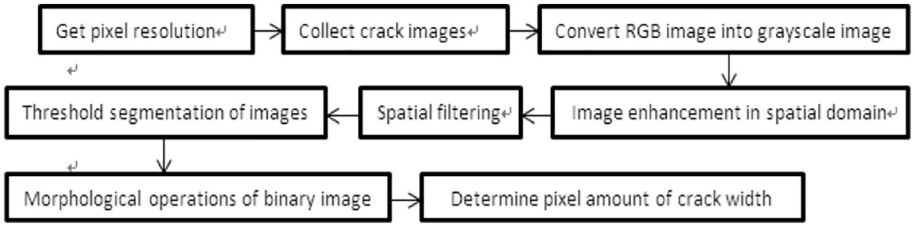

Fig. 1. Workflow of the identification of crack width in static image.